# Design and Analysis of an Empennage and Control Surfaces for Design Build Fly at Virginia Tech

Ryan Fisher[1]
[1] Kevin T. Crofton Department of Aerospace and Ocean Engineering, Blacksburg,

*Stability and control analysis is critical for the success of any aircraft, along with the many other subdisciplines. The general goal for stability and control is to provide the pilot with the proper control authority for flight through all mission phases, eliminating any undesirable responses of the aircraft. This paper looks to provide a study of stability and control for Virginia Tech's Design Build Fly competition aircraft. The optimization of the tail length, weight, and the moment are completed while defining the proper horizontal stabilizer characteristics such as airfoil and incidence angle to ensure static stability. Aileron sizing is completed to provide the pilot with significant roll authority. The associated control surface hinge moments generated from maneuvers are found using XFLR for manufacturing purposes. Lastly, a look at dynamic stability is provided with a brief look into future corrections to be made to the aircraft. In the future, a look into the proper sizing of the vertical stabilizer to counter crosswinds, along with the implementation of a feedback controller, will be conducted to ensure the success of this year's competition plane.*

**Keywords**: Stability and control, lateral stability, longitudinal stability, empennage

## 1 INTRODUCTION

The goal of this paper is to provide an in-depth analysis of topics relevant to stability and control for Design, Build, Fly (DBF) at Virginia Tech. Design Build Fly is tasked to create a banner towing, passenger-carrying, RC aircraft for The American Institute of Aeronautics and Astronautics (AIAA) 2020 Design Build Fly competition. The general competition rules and criteria for this aircraft will not be provided in this paper and can be found through resources from AIAA, however relevant requirements will be explained. Due to the nature of stability and control, the planform for Design Build Fly has been selected after thorough score optimization and aerodynamic analysis. Papers relevant to these other disciplines may be found for a deeper understanding of Virginia Tech's Design Build Fly preferred concept identification process. The results in the paper are explicitly dependent on the aerodynamics, score optimization, and CAD disciplines.

This study looks to provide the reader with an understanding of how to properly design and size the empennage for an RC aircraft while ensuring static stability. The control surfaces will also be sized for required performance levels and the associated moments created will be quantified for manufacturing use. Note, it is assumed that the reader has some familiarity with XFLR5, a program which used for aerodynamic and stability analysis, as it will be used for conducting simulations.

For a thorough overview of stability and control characteristics, the following sections of this paper are divided as follows. First, the planform being used to complete stability and control discipline related actions will be identified in detail for the reader to have a general overview of the desired aircraft. Next, the process of tail sizing for static stability and proper control authority will be provided. The aileron size for proper roll rate will be identified and control authority will be provided. Following, the moments generated due to control surfaces will be calculated for manufacturing use. Lastly, a look into dynamic stability will be completed to ensure perturbations during flight will

## 2 DEFINING THE PLANFORM

The planform selected and to be studied is a highly cambered, low aspect ratio, high capacity RC plane. An image of the aircraft can be found in Figure 1. The following information provided was found by the aerodynamic sub-team after optimization of the score for mission. All numbers come from XFLR simulations and basic aerodynamic calculations.

The span of the aircraft, limited by competition regulations, is $60in$. There is no limit on planform area, and therefore the mean aerodynamic chord (MAC) is $41.62in$ , providing a wing area of approximately $2{,}304in^2$. The airfoil used is the MH 112, providing high lift and a significant lift to drag ratio compared to other airfoils. Information regarding 2-D flow over the MH 112 can be found using AirfoilTools [1]. The root chord is $46in$ and a tip chord of $23in$. The taper on the aircraft does not occur until at half span, providing a rectangular planform for half the span and a taper ratio of 0.5 for the remainder of the span. The aspect ratio for this aircraft is 1.44. The coefficient of lift, $C_L$, for the planform during cruise of 0.495 and a coefficient of moment, $C_m$, of 0.305 during cruise conditions. The wing is mounted at a 6° angle of attack during cruise allowing for significant lift during the passenger mission. Cruise speed is assumed to be $65\frac{ft}{s}$ at this time. Note that while the lift generated during cruise is significant, it comes at the cost of moment coefficient, which will adversely affect the tail size of this aircraft.

*Figure 1. Air Vehicle 1 (AV1) at Kentland Farms*

With an explanation of the planform now provided, the analysis of tail sizing and its relation to static stability can be provided.

## 3 STATIC STABILITY (TAIL SIZING)

Using historical data, horizontal and vertical tail volume ratios, $V_H$ and $V_V$ respectively, were determined. As seen in Table A, located in the Appendix, the average horizontal tail volume ratio for DBF planes is 0.30. Table B (Nicolai) provides a look at general aviation aircraft, some of which are capable of towing banners. The average tail volume ratios for these aircraft are 0.77 and 0.05 for the horizontal and vertical tail volume ratios respectively. From this information along with experience from previous years, it was determined that a tail volume ratio of 0.5 was to be used.

The vertical tail volume ratio is of less interest currently, as generally RC pilots neglect rudder control compared to general aviation. Note however that while vertical size is not explored heavily in this paper; it will be considered in the future for optimal crosswind rejection. The vertical tail volume ratio selected for initial calculations and weighting was 0.05, based on historical data from Nicolai.

Historical RC aircraft have been found to use a horizontal stabilizer ratio of $\frac{2}{3}AR_W$, where $AR_W$ is the aspect ratio of the wing [2] [3]. However, due to the nature of the low aspect ratio aircraft, a horizontal aspect ratio of 0.96 would not be fitting. A horizontal aspect ratio of 3 was selected based on a historical DBF aircraft with a similar wing aspect ratio which scored second in the overall competition.

### 3.1 Optimizing Tail Size

To begin determining the optimized tail size, criteria must be established as to what is desired. Generally, weight and weighted are the biggest factors in sizing the tail when attempting to reach set tail volume ratios [3]. Note horizontal tail volume ratio, which is kept constant during optimization, is:

$$V_H = \frac{l_H S_H}{\bar{C} S}$$

The vertical tail volume ratio is given by:

$$V_V = \frac{l_V S_V}{b S}$$

Sadraey provides a method of reducing the wetted area of the aircraft, however, individual analysis is completed to optimize with respect to weight and moment arm. Wetted area/drag is minimal for RC aircraft as generally there is a thing carbon fiber boom extending from the wing to the tail, providing a minimal wetted area between the wing and tail. However, the weight is of high interest due to the desire of carrying more passengers for an improved score, and a minimized moment arm to keep CG as far forward as possible for increased static stability. Factors considered during the optimization include the change in carbon fiber boom length, landing gear weight, wire weight, horizontal stabilizer and vertical stabilizer size (dependent on tail volume ratio). Iterating over a length of $50in$-$300in$, measured from MAC quarter chord to horizontal quarter chord, the graph shown in Figure # can be created to find the optimal tail size and length. The plot shows tail moment arm in blue and total weight in red. The minimum weight occurs when the boom is extended $105in$. The minimum moment arm occurs with the tail length at $60in$. A tail position of $90in$ is selected as the moment arm does not change significantly between this point and its minima. Additionally, this is the aft limit manufacturing could currently allow the tail extended due to materials available for purchase. The optimized tail weight was found to be 2.66lbs at a length of $90in$ measured from quarter chord to quarter chord, with a tail horizontal tail area of $558.4in^2$, with span and chord of $40.93in$ and $13.64in$ respectively. The optimal vertical tail was constrained to have a chord of equal to $\frac{2}{3}c_H$. The surface area of the vertical stabilizer was computed to be $80.5in^2$ with a height of $8.85in$ and a chord of $9.1in$. Again, the values associated with the vertical stabilizer are recommended values, not strict requirements. The horizontal stabilizer size is a strict requirement to assist in guaranteeing static stability when selecting an airfoil later in the process.

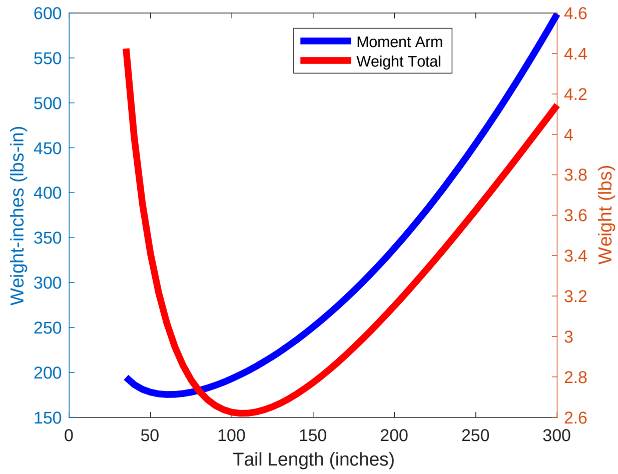


*Figure 2. Graph showing the optimized tail lengths for total eight and moment arm generated.*

### 3.2 Airfoil Selection for Static Stability

The next step in designing the tail is the selection of a tail configuration to best suit the mission. The three general tail configurations are fixed, adjustable, and all moving, all which are shown in Figure 3. to produce the proper downforce to counter the moment generated by the wing.

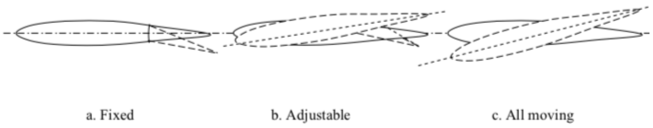


*Figure 3. General horizontal tail configurations (Cite Saudrey)*

A fixed configuration is selected for manufacturing purposes and to reduce the chances of inducing a tail stall. As Sadraey puts it, they are "lighter, cheaper and structurally easier to design" relative to other configurations.

Before selecting an airfoil and incidence angle for the tail, the downwash parameter, $\epsilon$, must be computed. This parameter is critical for our computation compared to other cases due to a large amount of lift being generated from the planform. The general equation for downwash is:

$$\epsilon = \epsilon_0 + \frac{\partial \epsilon}{\partial \alpha}\alpha_w$$

where,

$$\epsilon_0 = \frac{2C_{L_w}}{\pi AR}$$

And,

$$\frac{\partial \epsilon}{\partial \alpha} = \frac{2C_{L_{\alpha w}}}{\pi AR}$$

The downwash angle was found to be 0.49°. The coefficient of lift required by the tail can then be computed by:

$$C_{L_h} = \frac{C_{m_{0_{wf}}} + C_L(h - h_0)}{\eta_h + V_H}$$

Where $\eta_H$ is the tail efficiency, normally found to be between 0.85 and 0.95. The assumed value was 0.9. The remaining parameters were provided from the aerodynamics sub-team. The coefficient of lift required by the horizontal was found to be -0.373. The center of gravity, $CG$, was assumed to be at 11.5$in$, near quarter chord.

After exploring many airfoil options, an inverted NACA6412 was determined to be the optimal airfoil due to the downforce it can produce and its minimal likelihood of stalling compared to other airfoils. Figure 4 shows the $C_L$ vs. $\alpha$ curve for the horizontal stabilizer at cruise speed. Notice this occurs near -3.5° angle of attack.

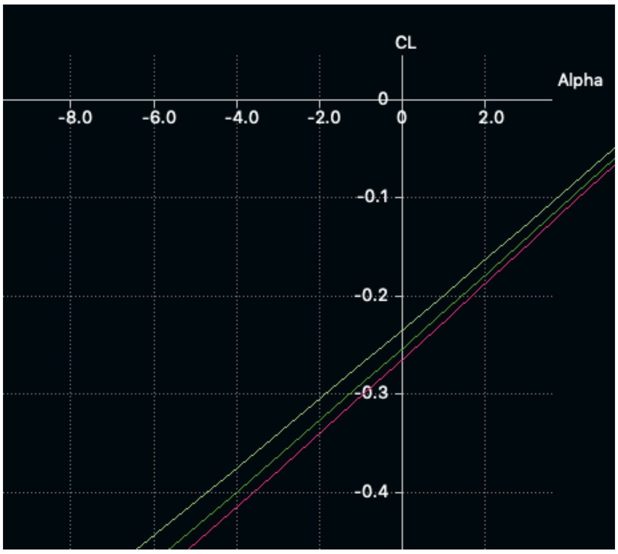


*Figure 4. Coefficient of lift versus angle of attack for NACA 6412 with span equal to 40in and chord equal to 13in.*

Factoring downwash angle, we can compute the required incidence angle (mounting angle) for the horizontal stabilizer.

$$i_h = \alpha_h + \epsilon - \alpha_f$$

Where $\alpha_f$ equals zero. The incidence angle is found to be approximately -3°. The tail is now ready for full implementation into XFLR5 for analysis.

Once the tail is implemented in XFLR5, VLM methods can be used to observe static stability via $C_{M_\alpha}$ and by determining the neutral point. With the $CG$ located at 11.5$in$, the following coefficient of moment and coefficient of lift graphs are generated for Air Vehicle 1 (AV1), as seen in Figures 5 and 6.

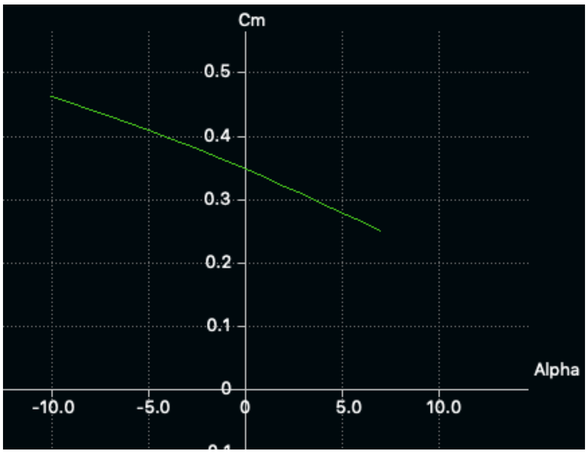


*Figure 5. Coefficient of moment versus angle of attack for Air Vehicle 1*

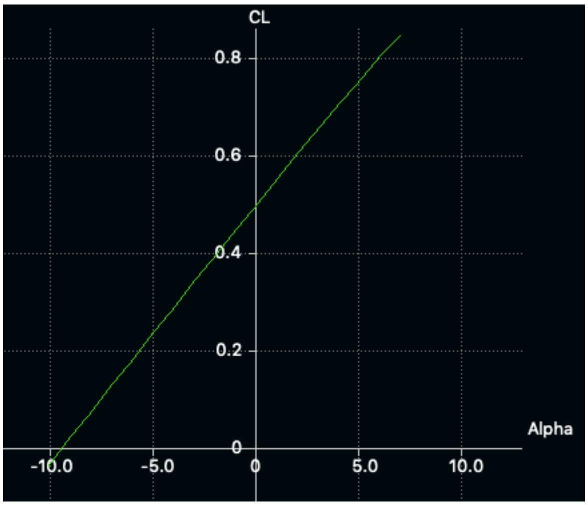


*Figure 6. Coefficient of lift versus angle of attack for Air Vehicle 1*

Using the simulation data from the previous figures, the neutral point is found to be located at $24.05in$, giving a static margin of 27%. This aircraft is statically stable in the lateral direction and has a tail that will provide sufficient downforce during flight conditions. The downforce provided is approximately $4.2lbs$.

## 4 AILERON SIZING

To size ailerons for a sufficient roll rate, the desired roll rate must be provided. Based on historical data, a roll rate near 100 degrees per second is desirable for RC aircraft. To build up to an understanding of roll rate and its dependent variables, some initial parameters will be defined.

From Woolsey [4], the change in lift due to change in aileron deflection is defined as:

$$C_{l_{\delta_a}} = \frac{\partial C_l}{\partial \delta_a} = \frac{2C_{L_{\alpha w}}\tau}{Sb}\int_{y1}^{y2} c(y)y\,dy$$

Where $c(y)$, the chord as a function of span, for the planform being analyzed can be represented as a piecewise function:

$$c(y) = \begin{cases} 3.83, & 0 < y < 1.25 \\ -1.53y + 5.75, & 1.25 < y < 2.5 \end{cases}$$

Where $c(y)$ and $y$ are measured in feet. Figure 7 shows how $c(y)$ is defined.

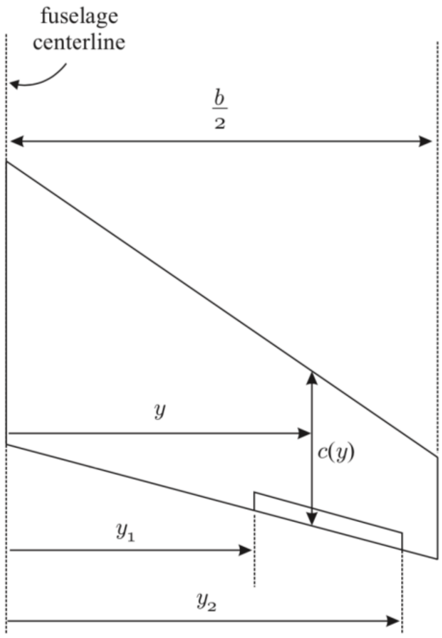


*Figure 7. Visual of c(y) is defined across a planform, with $y_1$ and $y_2$ defining start and end location of the aileron*

The control surface angle of attack effectiveness parameter, $\tau$, found using charts from Sadraey, was computed as 0.25 for 10% chord, 0.4 for 20% chord, and 0.52 for 30% chord. The roll rate can then be computed using:

$$P = -\frac{2V}{b}\frac{C_{l_{\delta_a}}}{C_{l_p}}\delta_a$$

Where $C_{l_p}$ is defined as the roll damping coefficient, computed to be 0.15 from charts found in Nicolai. The varying $\tau$, and maximum $\delta_a$, a roll rate of 124.3 degrees per second can be obtained with 10% chord aileron and 20° deflection of the aileron. To provide a roll rate, of 207.1, the ailerons can be deflected to 30.

## 5 CONTROL SURFACE MOMENTS

For manufacturing to install servos for changing control surface deflection, they must know how the magnitude of moment the servo will encounter. To quantify these moments, xflr5 provides means of finding hinge moments by simply altering the airfoil with a specified "flap".

### 5.1 Ailerons

Per the identification of the ailerons needed in the previous section, the corresponding moments will also be found. Implementing these in XFLR5 as new airfoils, with deflections of both +30° and -30°, the moments can be found. The aircraft must be tested at various angles of attack, as the maximum forces on the ailerons will not occur during straight and level flight. Figure 8 shows an image of the aircraft operating during cruise with ailerons deflected 30° at -10° angle of attack. Figure 9 shows the aircraft operating at +5° angle of attack.

The hinge moment generated by the right aileron with positive deflection (downwards), when operating at -10° angle of attack is 5.62$lbf.in$. The hinge moment generated by the left aileron with negative deflection (upward) at the same angle of attack, is 0.9862$lbf.in$. The hinge moments on the right and left aileron that occurs when pitched upwards at 5° angle of attack are 2.3$lbf.in$ and 3.98$lbf.in$ respectively. Therefore, the servos should be designed to the positive deflection in the downward pitched case, which has a maximum magnitude of 5.62$lbf.in$.

.

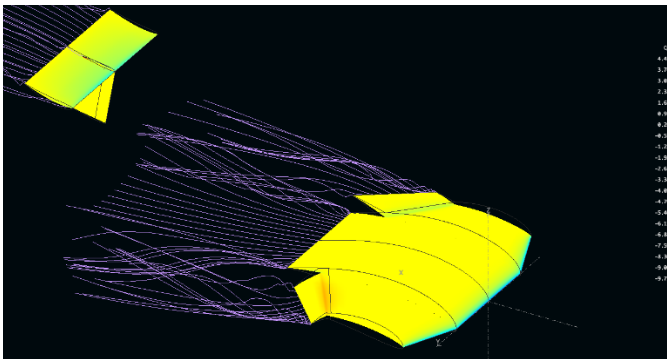

*Figure 8. Air Vehicle 1 cruising 65 ft/s at -10° angle of attack*

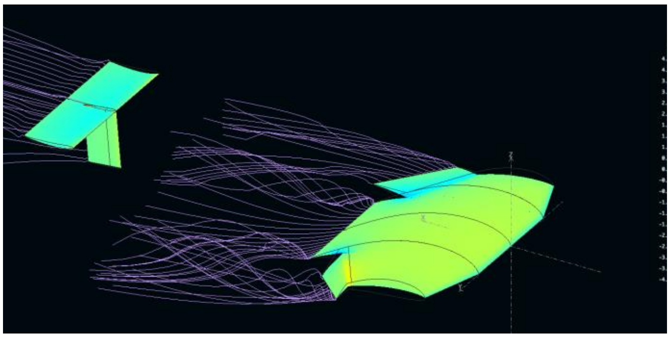

*Figure 9. Air Vehicle 1 cruising 65 ft/s at 5° angle of attack*

### 5.2 Elevator

From experimental testing using a foam plane, it was determined that the elevator size required was approximately 45% chord, a deflection of approximately 20°. This deflection angle is used to reduce the chances of stalling the horizontal stabilizer. Implementing "new" airfoils in XFLR5, with the flap starting at 55% chord, with a deflection of +20° and -20°, the hinge moments can be found. Figure 10 shows the horizontal stabilizer with an elevator deflection of -20°, effectively pitching the plane upwards.

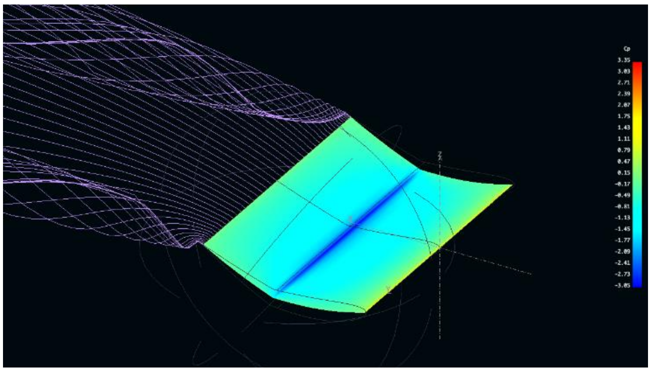

*Figure 10. Horizontal stabilizer (airfoil NACA6412) operating at 65 ft/s with -20° elevator deflection*

The hinge moments found for the elevator are as follows: 6.52$lbf.in$ for -20° deflection and 1.26$lbf.in$ for a +20° deflection while operating at 2° and 10° angle of attack respectively. These angles of attack corresponded to the maximum hinge moments for the respective elevator deflection. The angles of attack presented do not account for the incidence angle of the tail, and therefore are only representative of the tail in straight and level flight. Accounting for the incidence angle, the aircraft would have to be pitched to 5° and 13° angle of attack to achieve the maximum hinge moments. There is a significant difference in magnitude between the hinge moments, meaning that much more torque will be required by the servo to pitch the aircraft nose up. The servo should be designed again for the 6.52$lbf.in$ torque.

### 5.3 Rudder

The airfoil selected for the rudder is a NACA 0012 based on conventional use in RC aircraft. The rudder is not used significantly by the RC pilots compared to that of general aviation. This is due to the high reliance on ailerons and elevator for maneuverers, and approaches to runways are not required to be smooth nor coordinated. Therefore, convention drives the design of the rudder generally, resulting in a maximum 30° deflection with the rudder being 30% of the chord. Figure 11 shows an image of the rudder operating with a -30° deflection with yaw being 0°.

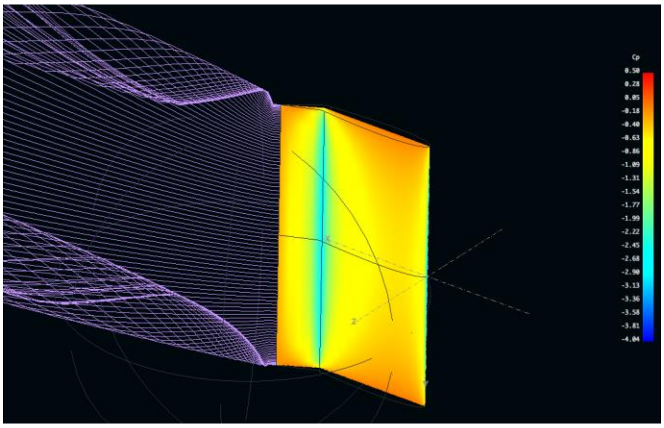

*Figure 11. Vertical stabilizer (airfoil NACA0012)) operating at 65 ft/s with -30° rudder deflection*

The maximum hinge moment generated by the rudder at -30° deflection was computed to be $0.68 lbf.in$. Note there is only one deflection computed as a +30° deflection would generate the same moment due to the symmetry of the airfoil.

## 6 DYNAMIC STABILITY

Running a dynamic stability test in XFLR5 with viscous effects, and the center of gravity located in the same position as all previous analyses can help determine if the aircraft can operate with perturbations mid-flight. From the CAD sub-team, the following moment of inertia matrix about the $CG$ was provided:

$$\begin{bmatrix} L_{xx} & L_{xy} & L_{xz} \\ L_{yx} & L_{yy} & L_{yz} \\ L_{zx} & L_{zy} & L_{zz} \end{bmatrix} = \begin{bmatrix} 14590 & -3.89 & -20.11 \\ -3.89 & 16257 & -406.53 \\ -20.11 & -406.53 & 1989.21 \end{bmatrix}$$

These values were used in XFLR5 to conduct a dynamic stability test, which tests longitudinal and lateral stability. The longitudinal dynamic stability tests address two symmetric phugoid modes and two symmetric short period modes (one which is sometimes called the long period). The lateral dynamic stability tests look at one spiral mode, one roll damping mode, and two Dutch roll modes. The results are shown in Tables 1-4.

| Mode | Eigenvalue |
|---|---|
| **Phugoid** | -7.382+ 0i |
| **Phugoid** | -5.473+ 0i |
| **Short Period** | -0.09557+ -1.008i |
| **Short Period** | -0.09557+ 1.008i |

*Table 1. Longitudinal stability eigenvalues*

| $\zeta$ | $\omega_n$ | $\zeta\omega$ | $t_{half}$ | $N_{half}$ |
|---|---|---|---|---|
| 1 | 2.422 | 2.422 | 0.28489 | 0 |
| 1 | 0.3491 | 0.3491 | 1.9765 | 0 |
| 0.95722 | 2.2941 | -2.196 | 0.31421 | 0.033195 |
| 0.95722 | 2.2941 | -2.196 | 0.31421 | 0.033195 |

*Table 2. Longitudinal stability analysis*

| Mode | Eigenvalue |
|---|---|
| **Spiral** | -2.422+ 0i |
| **Roll Damping** | -0.3491+ 0i |
| **Dutch Roll** | 2.196+ -0.6638i |
| **Dutch Roll** | 2.196+ 0.6638i |

*Table 3. Lateral stability eigenvalues*

| $\zeta$ | $\omega_n$ | $\zeta\omega$ | $t_{half}$ | $N_{half}$ |
|---|---|---|---|---|
| 1 | 7.382 | 7.382 | 0.093471 | 0 |
| 1 | 5.473 | 5.473 | 0.12607 | 0 |
| 0.094388 | 1.0125 | 0.09557 | 7.2198 | 1.1583 |
| 0.094388 | 1.0125 | 0.09557 | 7.2198 | 1.1583 |

*Table 4. Lateral stability analysis*

The results show great longitudinal stability, with all eigenvalues containing negative real part. However, the lateral stability is lacking with the Dutch roll eigenvalues showing significant positive real part. This may cause issues during flight test if large perturbations exist. Also, notice that the corresponding damping ratio is very low (less than 0.1). Methods of reducing the effect of the Dutch roll instability, or even eliminating it, will be researched moving forward. Upon initial findings, having the center of gravity above the wings and a larger vertical stabilizer may be solutions as it will improve the damping ratio; however, no claim can be made regarding these solutions yet. If physical adjustments to the aircraft do not significantly improve this instability, a feedback controller will be considered. XFLR5 does provide the stability derivates and corresponding state matrix, along with the input matrix. After a brief analysis, a feedback controller is possible as the unstable eigenvalues are controllable.

## 7 CONCLUSION

In conclusion, a study has been completed successfully on the design and analysis of an empennage and control surfaces for Design Build Fly's 2019-2020 competition plane. The initial planform was defined in order for the reader to have a better understanding of the aircraft. The tail size was optimized using a weight and moment analysis which factored in boom material, landing gear, wires, and size of the vertical and horizontal stabilizers. Other factors included historical data regarding aspect ratios and tail volume ratios. A tail configuration was then chosen based on general knowledge of historical usage. Next, an airfoil was selected after computing the coefficient of lift needed by the horizontal stabilizer, $C_{L_H}$. Static stability was then proven after implementation in XFLR5. The ailerons were sized to provide the required roll authority to the pilot based on past RC aircraft. Control surface hinge moments were identified for the manufacturing sub-team to allow the installation of servos with sufficient torque for operation during all flight envelopes. Lastly, a study on longitudinal and lateral dynamic stability was completed using XFLR5. It was shown that the aircraft is not dynamically stable in the Dutch roll mode, and further investigation is needed. A feedback controller was also identified as a viable option due to the unstable eigenvalues being controllable.

Moving forward, the vertical stabilizer will be sized to counter cross-winds that could arise in the mission profile. As well, research into a solution eliminating Dutch roll instability will be complete, with an exploration of a feedback controller or other options presented by colleagues. Completion of these two tasks will ensure the team is competition ready, specifically in the stability and control discipline.

## 8 ACKNOWLEDGMENTS

The author would like to thank Design Build Fly for the opportunity to perform the role of Stability and Control Engineer for this year's competition. As well, thank you to Craig Woolsey for establishing a foundation for students regarding the fundamentals stability and control and the associated control laws.

# 9 APPENDIX

| Name | Span | Chord | S | L | AreaTail | Tail Camber | V_H |
|---|---|---|---|---|---|---|---|
| Stick Plane | 43 | 6.5 | 279.5 | 12 | 52 | Neutral | 0.34347 |
| Water plane | 51 | 8 | 408 | 7 | 65 | Cambered Tail | 0.1394 |
| Gatorade | 43 | 9 | 387 | 10 | 94.5 | Neutral | 0.271318 |
| Trainer | 51 | 8.5 | 433.5 | 11 | 108 | Neutral | 0.32241 |
| VT19 | 90 | 14 | 1260 | 26 | 285 | Cambered Tail | 0.420068 |
| Flappybird | 29 | 8 | 232 | 10 | 28.5 | Neutral | 0.153556 |
| Atlas | 18 | 15 | 270 | 4 | 29.75 | Cambered Tail | 0.029383 |
| SAE Orange | 64 | 12 | 768 | 18 | 156 | Neutral | 0.304688 |
| Reaper Mini | 26 | 3.5 | 91 | 3.2 | 23.75 | Neutral | 0.238619 |
| Stick Plane | 40 | 8 | 320 | 22 | 99 | Neutral | 0.850781 |
| AVG | 45.5 | 9.25 | 420.875 | 12.32 | 94.15 | - | 0.297945 |

*Table A. Horizontal* Tail Volume Coefficients for Historical DBF Aircraft

| PLANE | ENGINES | CHT | CVT |
|---|---|---|---|
| **CESSNA SKYWAGON** | 1 | 0.92 | 0.046 |
| **CESSNA CARDINAL** | 1 | 0.6 | 0.038 |
| **CESSNA SKYLANE** | 1 | 0.71 | 0.047 |
| **PIPER CHEROKEE** | 1 | 0.61 | 0.037 |
| **BELLANCA SKYROCKET** | 1 | 0.61 | 0.037 |
| **GRUMMAN TIGER** | 1 | 0.76 | 0.024 |
| **CESSNA 310** | 2 | 0.95 | 0.063 |
| **CESSNA 402** | 2 | 1.07 | 0.08 |
| **CESSNA 414** | 2 | 0.93 | 0.071 |
| **PIPER 414** | 2 | 0.84 | 0.056 |
| **PIPER CHIEFTAIN** | 2 | 0.72 | 0.055 |
| **PIPER CHEYENNE** | 2 | 0.85 | 0.045 |
| **BEECH DUCHESS** | 2 | 0.67 | 0.053 |
| **BEECH DUKE** | 2 | 0.64 | 0.06 |
| **AVERAGE** | | 0.77714286 | 0.05085714 |

*Table B.* Tail Volume Coefficients for Light Reciprocating–Propeller Aircraft [5]

## 10 WORKS CITED

[1] "Airfoil Tools," 2019. [Online]. Available: http://airfoiltools.com/airfoil/details?airfoil=mh112-il. [Accessed 14 December 2019].

[2] RIT, "MSD: SAE Aero Aircraft Design & Build".

[3] M. H. Sadraey, Aircraft Design: A Systems Engineering Approach, West Sussex: John Wiley & Sons, 2013.

[4] C. A. Woolsey, Topic 3: Lateral-Directional Static Stability & Control, Blacksburg, 2019.

[5] L. M. Nicolai and G. E. Carichner, Fundamentals of Aircraft and Airship Design, Vols. I - Aircraft Design, J. A. Schetz, Ed., Reston, Virginia: American Institute of Aeronautics and Astronautics, 2010.